Technical Report # MBS99-5-UIC
Department of Mechanical Engineering
University of Illinois at Chicago

December 1999

A FINITE ELEMENT STUDY OF THE GEOMETRIC CENTRIFUGAL STIFFENING EFFECT

Marcello Berzeri
Ahmed A. Shabana

Department of Mechanical Engineering
University of Illinois at Chicago
842 West Taylor Street
Chicago, IL 60607-7022

This research was supported by the U.S. Army Research Office, Research Triangle Park, NC, and, in part, by the National Science Foundation.

REPORT DOCUMENTATION PAGE

Form Approved
OMB NO. 0704-0188

1. AGENCY USE ONLY *(Leave blank)*	2. REPORT DATE	3. REPORT TYPE AND DATES COVERED
	December 1999	Technical Report

4. TITLE AND SUBTITLE

A Finite Element Study of the Geometric Centrifugal Stiffening Effect

5. FUNDING NUMBERS

DAAG55-97-1-0303

6. AUTHOR(S)

Marcello Berzeri
Ahmed A. Shabana

7. PERFORMING ORGANIZATION NAMES(S) AND ADDRESS(ES)

University of Illinois at Chicago
Chicago, IL 60607-7022

8. PERFORMING ORGANIZATION REPORT NUMBER

9. SPONSORING / MONITORING AGENCY NAME(S) AND ADDRESS(ES)

U.S. Army Research Office
P.O. Box 12211
Research Triangle Park, NC 27709-2211

10. SPONSORING / MONITORING AGENCY REPORT NUMBER

ARO 35711.21-EG

11. SUPPLEMENTARY NOTES

The views, opinions and/or findings contained in this report are those of the author(s) and should not be construed as an official Department of the Army position, policy or decision, unless so designated by other documentation.

12a. DISTRIBUTION / AVAILABILITY STATEMENT

Approved for public release; distribution unlimited.

12 b. DISTRIBUTION CODE

13. ABSTRACT *(Maximum 200 words)*

ABSTRACT IN TECHNICAL REPORT

14. SUBJECT TERMS

15. NUMBER IF PAGES

16. PRICE CODE

17. SECURITY CLASSIFICATION OR REPORT	18. SECURITY CLASSIFICATION OF THIS PAGE	19. SECURITY CLASSIFICATION OF ABSTRACT	20. LIMITATION OF ABSTRACT
UNCLASSIFIED	UNCLASSIFIED	UNCLASSIFIED	UL

ABSTRACT

The finite element absolute nodal coordinate formulation is used in this investigation to study the centrifugal stiffening effects on rotating two-dimensional beams. It is demonstrated that the geometric stiffening effects can be automatically accounted for in the above mentioned finite element formulation by using an expression for the elastic forces obtained with a general continuum mechanics approach. The Hill equation that governs the vibration of the rotating beam is obtained in terms of a set of generalized coordinates that describe the beam displacements and slopes. Under the assumption of small deformation, the Hill equation is linearized, and the complete solution is obtained and used to demonstrate analytically that such a solution does not exhibit instabilities as the angular velocity of the beam increases. The results obtained using this finite element procedure are compared with the results reported in the literature.

1 INTRODUCTION

The dynamic behavior of rotating beams has been the subject of interest in many engineering applications such as helicopter blades, flexible robot arms, turbine blades and turbo-engine blades. In many of these applications, flexible beams are rotating at high angular velocities, and as a result the effects of the inertia centrifugal and Coriolis forces becomes significant. Furthermore, the centrifugal forces lead to a higher bending stiffness of the beam as compared to the case of a non-rotating beam. The rotation of the beam produces a geometric stiffening effect that is referred to in the literature as the centrifugal stiffening. Extensive research has been conducted in the past in order to properly account for this effect.

In the field of flexible multibody dynamics, the most widely used approach is the floating frame of reference formulation. In this formulation, a reference coordinate system is assigned to each body in the system. The motion of this coordinate system (also called shadow frame) describes the gross motion of the body. Small deformations are measured with respect to this body coordinate system, and the total motion of the body is determined as the sum of the gross motion and the small deformation. The floating frame of reference formulation has been proved to be efficient in the analysis of large displacement/small deformation problems. For these problems and until recently, linear strain-displacement relationships were considered sufficient for the description of the small deformation. Kane et al [11] showed that under the described conditions, the results obtained using the floating frame of reference formulation incorrectly exhibit instability that is not present in the physical model. Simo and Vu-Quoc [18] demonstrated that, in the case of a rotating beam, linear theories predict inadmissible destabilization effects, even for extremely stiff beams. They showed that a second-order theory solves the problem. While the cause for this instability has not been completely explained, several methods have been proposed to successfully solve the problem [3, 4, 6, 11, 18, 19].

In general, it is believed that the instability of the elastically linear models is due to

the neglect of the coupling between the longitudinal and transverse displacements, so that the bending deformation of the beam does not cause any variation in the longitudinal displacement [11]. Wu and Haug [21] presented a solution based on substructuring the flexible bodies, and used bracket joints to impose the nonlinear connectivity conditions between the substructures. El-Absy and Shabana [6] showed that including the effect of longitudinal displacement caused by bending in the expression of the inertia forces leads to a consistent model that automatically accounts for the stiffening effect. Wallrapp and Schwertassek [14, 19] showed that it is possible to neglect the longitudinal displacements, which are indeed very small, and introduce the stiffening effect as a pre-stressed reference condition.

In addition to these important investigations that are essentially focused on multibody dynamics problems, many other authors examined the frequencies and vibration modes of centrifugally stiffened beams [8, 9, 12, 13, 20, 23, 24] . In many cases, the beam is modelled as a continuum and the equations of motion are solved using different techniques. For example, Schilhansl [13] used the method of successive approximation, while Wright et al [20] used the method of Frobenius to solve for the exact frequencies and mode shapes. The assumed mode method, however, remains the most widely used approach [8, 9, 23, 24], despite the fact that the finite element method has been considered by several authors as demonstrated by the work of Putter and Manor [12].

In this paper the problem of centrifugal stiffening will be addressed using a new finite element formulation for flexible multibody dynamics. The absolute nodal coordinate formulation, which was recently introduced [16], will be used in this investigation. This is a non-incremental finite element procedure, that employs global coordinates as nodal degrees of freedom. Furthermore, two slopes instead of one angle are used to describe the rotation of the cross section of an Euler-Bernoulli beam element. This choice of the coordinates leads to isoparametric elements. The use of the absolute nodal coordinate formulation in the analysis of flexible multibody systems has been demonstrated in several previous publica-

tions [5, 7, 22]. The equivalence between this formulation and the floating frame of reference formulation was also demonstrated [1, 17]. In the first presentation of this method, the expression of the elastic forces was obtained using a linear strain-displacement relationship, and for this reason centrifugal stiffening effects were not accounted for. More recently, a continuum mechanics approach was proposed to calculate the elastic forces [2]. It is the purpose of this paper to demonstrate that this new method automatically takes into account the stiffening effects. The absolute nodal coordinate formulation will then be used to calculate the natural frequencies and mode shapes of a rotating beam. Several numerical examples are provided, and the results are compared with the results reported by different authors. The natural frequencies for different configurations of a rotating beam are also reported in this paper.

2 FORMULATION OF THE INERTIA AND ELASTIC FORCES

In the non-incremental absolute nodal coordinate formulation [16], the nodal coordinates of the elements are defined in a fixed inertial coordinate system, and consequently no coordinate transformation is required, the mass matrix is constant and the Coriolis and centrifugal forces are identically equal to zero. In the absolute nodal coordinate formulation of non-shear deformable elements, no infinitesimal or finite rotations are used as nodal coordinates and no assumption on the magnitude of the element rotations is made.

In this investigation, two dimensional Euler-Bernoulli beam elements are considered. Each element is assumed to be slender, so that its configuration can be uniquely described by the geometrical configuration of the neutral axis. The global position vector $\mathbf{r}$ of an arbitrary point P on the neutral axis is defined in terms of the nodal coordinates and the

element shape function, as

$$\mathbf{r} = \begin{bmatrix} r_1 \\ r_2 \end{bmatrix} = \mathbf{S}\mathbf{e}, \tag{1}$$

where $\mathbf{S}$ is the global shape function which has a complete set of rigid body modes, and $\mathbf{e}$ is the vector of element nodal coordinates:

$$\mathbf{e} = \begin{bmatrix} e_1 & e_2 & e_3 & e_4 & e_5 & e_6 & e_7 & e_8 \end{bmatrix}^{\mathrm{T}}. \tag{2}$$

This vector of absolute nodal coordinates includes the global displacements

$$e_1 = r_1|_{x=0}, \quad e_2 = r_2|_{x=0}, \quad e_5 = r_1|_{x=l}, \quad e_6 = r_2|_{x=l}, \tag{3}$$

and the global slopes of the element nodes, that are defined as

$$e_3 = \left.\frac{\partial r_1}{\partial x}\right|_{x=0}, \quad e_4 = \left.\frac{\partial r_2}{\partial x}\right|_{x=0}, \quad e_7 = \left.\frac{\partial r_1}{\partial x}\right|_{x=l}, \quad e_8 = \left.\frac{\partial r_2}{\partial x}\right|_{x=l}. \tag{4}$$

Here x is the coordinate of an arbitrary point on the element in the undeformed configuration, and l is the original length of the beam element. The two end points of the element are denoted as A and B, where $x = 0$ at point A, and $x = l$ at B, as shown in Fig. 1. A cubic polynomial is employed to describe both components of the displacements. Therefore, the global shape function $\mathbf{S}$ can be written as

$$\mathbf{S} = \begin{bmatrix} s_1 & 0 & s_2 l & 0 & s_3 & 0 & s_4 l & 0 \\ 0 & s_1 & 0 & s_2 l & 0 & s_3 & 0 & s_4 l \end{bmatrix}, \tag{5}$$

where the functions $s_i = s_i(\xi)$ are defined as

$$s_1 = 1 - 3\xi^2 + 2\xi^3, \quad s_2 = \xi - 2\xi^2 + \xi^3, \quad s_3 = 3\xi^2 - 2\xi^3, \quad s_4 = \xi^3 - \xi^2, \tag{6}$$

and $\xi = x/l$. It can be shown that the preceding shape function contains a complete set of rigid body modes that can describe arbitrary rigid body translational and rotational displacements.

The kinetic energy of a beam element can be defined as

$$T = \frac{1}{2}\int_V \rho \dot{\mathbf{r}}^{\mathrm{T}}\dot{\mathbf{r}} dV, \tag{7}$$

where ρ and V are, respectively, the density and the volume of the beam in the current configuration. Using Euler-Bernoulli beam assumptions, it is possible to write Eq. 7 as

$$T = \frac{1}{2}\dot{\mathbf{e}}^{\mathrm{T}}\mathbf{M}\dot{\mathbf{e}}, \tag{8}$$

where the explicit form of the mass matrix $\mathbf{M}$ is given in the appendix.

Following Euler-Bernoulli beam theory, the strain energy can be written as

$$U = \frac{1}{2}\int_0^l [EA\varepsilon_l^2 + EI\kappa^2] dx, \tag{9}$$

where ε_l represents the longitudinal deformation, and κ is the curvature of the beam. From the expression of the strain energy, the vector $\mathbf{Q}_k$ of the elastic forces can be obtained as $\mathbf{Q}_k = (\partial U/\partial \mathbf{e})^{\mathrm{T}}$. This vector can then be written as the product of a stiffness matrix $\mathbf{K}$ and the vector of nodal coordinates, as $\mathbf{Q}_k = \mathbf{K}\mathbf{e}$. Different approaches can be followed in order to further develop the expression of the strain energy U and express it in terms of the generalized coordinates. From this expression the stiffness matrix $\mathbf{K}$ can be defined. In [16], a local element coordinate system is introduced to define the beam deformation. This approach results in a highly nonlinear expression for the elastic forces. It is shown that different local element coordinate systems lead to the same results [1], and more important for the subject of this paper is the fact that the stiffness matrix $\mathbf{K}$, obtained by introducing a local element coordinate system and a linear strain-displacement relationship, leads to the instability problem when the angular velocity of the beam reaches a critical value.

Using a nonlinear continuum mechanics approach, a different expression for the stiffness matrix $\mathbf{K}$ can be obtained [2]. The stiffness matrix can be written as

$$\mathbf{K} = \mathbf{K}_l + \mathbf{K}_t, \tag{10}$$

where $\mathbf{K}_l$ is the nonlinear stiffness matrix due to the longitudinal deformation of the beam, while $\mathbf{K}_t$ is the stiffness matrix due to the transverse deformation. The complete expressions for these stiffness matrices are given in the appendix of this paper.

The vector $\mathbf{Q}$, which contains the generalized external forces, including the gravity force, can be defined using the virtual work as

$$\delta W = \mathbf{Q}^{\mathrm{T}} \delta \mathbf{e}, \tag{11}$$

and using the previous expressions of the kinetic energy, strain energy, and the virtual work, the dynamic equations of the finite element can be obtained in a matrix form as follows:

$$\mathbf{M}\ddot{\mathbf{e}} + \mathbf{K}\mathbf{e} = \mathbf{Q}. \tag{12}$$

The solution of this matrix equation, which is obtained using the absolute nodal coordinate formulation, is compared in the following section with other methods that account for the effect of the geometric centrifugal stiffening.

3 OTHER METHODS

Several other methods that account for the effect of the geometric centrifugal stiffening were proposed. Among these methods are the ones proposed by Wallrapp and Schwertassek [14, 19] and Wu and Haug [21]. Wallrapp and Schwertassek [19] showed that it is possible to neglect the small longitudinal displacements and introduce the geometric centrifugal stiffening effect as a pre-stressed reference condition. Wu and Haug [21] divided the structure into smaller substructures which are rigidly connected using algebraic constraint equations. These algebraic equations can be augmented to the differential equations of motion using the technique of Lagrange multipliers, or can be used to eliminate dependent variables.

In this section, some of the results obtained using the absolute nodal coordinate formulation are compared with the two above mentioned methods, using two of the examples

reported in Refs. 19 and 21. Both examples consider the problem of a rotating beam. In Ref. 19 the beam is eccentrically suspended (eccentricity = 1 m), while in Ref. 21 the beam is rotating about an axis passing through one of its ends. The data for these two examples are presented in Table 1. The rotation of the beams is specified, and the equation that defines the angle of rotation of the beam is assumed in the following form:

$$\theta(t) = \begin{cases} \frac{\Omega}{T}\left[\frac{t^2}{2} + \left(\frac{T}{2\pi}\right)^2\left(\cos\frac{2\pi t}{T} - 1\right)\right] & t < T \\ \Omega\,(t - T/2) & t \geq T \end{cases} \tag{13}$$

Equation 13 represents a spin-up maneuver starting at time $t = 0$ and ending at time $t = T = 15$ sec; at this ending time a constant angular velocity Ω is reached. The steady-state value Ω of the angular velocity is equal to 6 rad/s in the example of Ref. 19, and to 2 and 4 rad/s in the examples of Ref. 21. In the comparative study presented in this section, two absolute nodal coordinate formulation models are used. In the first model, a linear strain-displacement relationship is used, and the expression of the elastic forces is derived using a local element coordinate system [16]. This model will be referred to in this investigation as Model 0. The second model, denoted as Model A (which corresponds to Model III of Ref. 2), is based on a continuum mechanics approach, and employs a nonlinear strain-displacement relationship. No local element coordinate system is used in formulating the elastic forces. Yet, the expression of the elastic forces obtained for Model A is much simpler than the expression of the elastic forces of Model 0 as previously demonstrated [2].

Figures 2 and 3 show the tip deflection and the free-end rotation, respectively, of the eccentrically suspended beam investigated by Wallrapp and Schwertassek [19]. The results of Model A are almost identical to the results of Case 6 of Ref. 19, which, for this reason, are not shown. Figures 4 and 5 show the tip deflection of the rotating beam subject to a spin-up maneuver with steady-state angular velocities of 2 rad/s and 4 rad/s, respectively. This is the example presented in Ref. 21. The results of the absolute nodal coordinate formulation are compared to the results presented in Ref. 21 using a 6 substructure beam.

It is important to point out that all the results of the absolute nodal coordinate formulation in Figs. 2-5 are obtained using only two elements, and for the case of Model A the degree of accuracy is very high. Increasing the number of elements, the results of Model 0 improve significantly, as this is conceptually equivalent to further substructuring the beam. However, as previously demonstrated [1], there always exists a critical value of the angular velocity beyond which the rotating beam exhibits instability when Model 0 is used. This critical value depends on the number of elements used to discretize the beam. Figures 6 and 7 show the effect of the number of elements on the stability of the beam when Model 0 is used. In these figures, the beam dimensions and material properties are the same as used by Wu and Haug [21]. For the models used in Fig. 6 the steady-state angular velocity is equal to 10 rad/s, and the one-element mesh leads to instability using Model 0. Increasing the number of elements to ten, the results of Model 0 and Model A are almost identical. In Fig. 7, the constant value of the angular velocity Ω is increased to 40 rad/s. As demonstrated by the results presented in this figure, two elements are not sufficient when Model 0 is used, while the solution obtained using Model A remains stable.

It appears from these preliminary numerical results that the elastic force model obtained using a continuum mechanics approach (Model A) automatically accounts for the centrifugal stiffening effect. It is important, however, to provide an analytical proof of this fact. Due to the high non-linearity of the problem, a general proof is difficult to obtain. For this reason, we will limit our analysis to the important case of small deformation. This case is important for the following two reasons: 1) it covers a vast class of engineering applications; and 2) the neglect of stiffening effects leads to incorrect results regardless of the amount of deformation, as previously pointed out by Simo and Vu-Quoc [18], who showed that the solution exhibits instability even for extremely stiff beams, which undergo only very small deformations. It is, therefore, the purpose of the next section to demonstrate that the formulation based on Model A accounts for the centrifugal stiffening effect. Consequently, such a formulation

does not lead to any instability, regardless of the value of the angular velocity of the beam element. Several numerical examples are presented in Section 7 in order to compare the results of the absolute nodal coordinate formulation with those obtained by other authors.

4 ROTATION OF A CANTILEVER BEAM

In this section, the elastic force Model A, equivalent to Model III introduced in [2] for studying small deformation problems, is used to analyze the stability of the motion of a rotating cantilever beam. The study model is shown in Fig. 8, and consists of a cantilever beam rigidly connected to a rigid hub. A tip mass m_t is attached to the free end of the beam. The rigid hub is assumed to rotate at a constant angular velocity Ω.

First, the case in which the beam is represented using only one finite element is considered. In this case, the configuration of the beam is specified using the eight nodal coordinates

$$\mathbf{e} = \begin{bmatrix} e_1 & e_2 & e_3 & e_4 & e_5 & e_6 & e_7 & e_8 \end{bmatrix}^{\mathrm{T}}, \tag{14}$$

and the total length L of the beam is equal to the length l of the element. The equations of motion for the rotating beam and the tip mass have the matrix form

$$(\mathbf{M} + \mathbf{M}_t)\ddot{\mathbf{e}} + \mathbf{K}\mathbf{e} = \mathbf{Q}_r, \tag{15}$$

where $\mathbf{M}$ is the mass matrix of the beam, $\mathbf{M}_t$ is the mass matrix associated with the tip mass, $\mathbf{K}$ is the stiffness matrix which can be written using the sum $\mathbf{K}_l + \mathbf{K}_t$ as previously discussed, and $\mathbf{Q}_r$ is the vector of the generalized forces that include the constraint forces due to the rigid joint between the beam and the hub. These rigid-joint constraints define a constraint force whose components are P_x and P_y, and a constraint moment Γ. Using the absolute coordinates, the virtual work of this force and moment is $\delta W_r = P_x \delta e_1 + P_y \delta e_2 + \Gamma \delta\theta = \mathbf{Q}_r^{\mathrm{T}} \delta\mathbf{e}$, where the virtual variation of θ is [16]:

$$\delta\theta = \frac{e_3 \delta e_4 - e_4 \delta e_3}{e_3^2 + e_4^2}. \tag{16}$$

Hence, the expression of $\mathbf{Q}_r$ is given by

$$\mathbf{Q}_r = \left[\begin{array}{cccccccc} P_x & P_y & \frac{-e_4}{e_3^2+e_4^2}\Gamma & \frac{e_3}{e_3^2+e_4^2}\Gamma & 0 & 0 & 0 & 0 \end{array} \right]^{\mathrm{T}}, \tag{17}$$

where P_x, P_y and Γ are unknown reaction components. In this analysis, the rotation of the hub is specified, and its motion is not the subject of our investigation. As a result of the hub rotation, $e_1 = R\cos\Omega t$, $e_2 = R\sin\Omega t$ and $\theta = \Omega t$, where Ω is a constant.

At this point, a new set of coordinates q_i is introduced. This new set completely defines the configuration of the beam and is given by

$$\mathbf{q} = \left[\begin{array}{ccccc} q_1 & q_2 & q_3 & q_4 & q_5 \end{array} \right]^{\mathrm{T}}, \tag{18}$$

where

$$q_1 = \left.\frac{\partial \eta_1}{\partial x}\right|_{x=0}, \quad q_2 = \eta_1|_{x=l}, \quad q_3 = \eta_2|_{x=l}, \quad q_4 = \left.\frac{\partial \eta_1}{\partial x}\right|_{x=l}, \quad q_5 = \left.\frac{\partial \eta_2}{\partial x}\right|_{x=l}, \tag{19}$$

and where η_1,η_2 are the coordinates of an arbitrary point on the beam defined with respect to a beam coordinate system rigidly attached to point A. Note that this local beam coordinate system has a constant angular velocity Ω, as shown in Fig. 9. Note also that in Eq. 18, only five coordinates are required due to the constraints that define the rigid joint between the beam and the hub.

The relationship between the absolute nodal coordinates $\mathbf{e}$ and the new set of coordinates $\mathbf{q}$ is given by

$$\mathbf{e} = \mathbf{B}\mathbf{q} + \mathbf{e}_r, \tag{20}$$

where $\mathbf{B}$ is the matrix

$$\mathbf{B} = \begin{bmatrix} 0 & 0 & 0 & 0 & 0 \\ 0 & 0 & 0 & 0 & 0 \\ \cos\Omega t & 0 & 0 & 0 & 0 \\ \sin\Omega t & 0 & 0 & 0 & 0 \\ 0 & \cos\Omega t & -\sin\Omega t & 0 & 0 \\ 0 & \sin\Omega t & \cos\Omega t & 0 & 0 \\ 0 & 0 & 0 & \cos\Omega t & -\sin\Omega t \\ 0 & 0 & 0 & \sin\Omega t & \cos\Omega t \end{bmatrix}, \tag{21}$$

and $\mathbf{e}_r$ is the vector

$$\mathbf{e}_r = R \begin{bmatrix} \cos\Omega t & \sin\Omega t & 0 & 0 & \cos\Omega t & \sin\Omega t & 0 & 0 \end{bmatrix}^{\mathrm{T}}. \tag{22}$$

Because of the structure of the matrix $\mathbf{B}$ and the vector $\mathbf{e}_r$, differentiation with respect to time leads to $\ddot{\mathbf{B}} = -\Omega^2\mathbf{B}$ and $\ddot{\mathbf{e}}_r = -\Omega^2\mathbf{e}_r$. As a result, the vector of absolute nodal accelerations can be written as

$$\ddot{\mathbf{e}} = \mathbf{B}\ddot{\mathbf{q}} + 2\dot{\mathbf{B}}\dot{\mathbf{q}} - \Omega^2\mathbf{B}\mathbf{q} - \Omega^2\mathbf{e}_r. \tag{23}$$

Using Eqs. 20 and 23, Eq. 15 can be written in terms of the independent coordinates q_i only. Substituting Eqs. 20 and 23 into Eq. 15 and pre-multiplying by $\mathbf{B}^{\mathbf{T}}$ results in

$$\overline{\mathbf{M}}\ddot{\mathbf{q}} + \overline{\mathbf{C}}\dot{\mathbf{q}} + (\overline{\mathbf{K}} - \Omega^2\overline{\mathbf{M}})\mathbf{q} = \overline{\mathbf{F}}_m. \tag{24}$$

Note that $\mathbf{B}^{\mathbf{T}}\mathbf{Q}_r = \mathbf{0}$, which is a direct consequence of expressing the dynamic relationships in terms of the degrees of freedom. Using the definition of the mass and stiffness matrices given in the appendix, the matrices $\overline{\mathbf{M}}$ and $\overline{\mathbf{C}}$ that appear in Eq. 24 can be written more

explicitly as

$$\overline{\mathbf{M}} = \mathbf{B}^{\mathbf{T}}(\mathbf{M}+\mathbf{M_t})\mathbf{B} = \begin{bmatrix} \frac{ml^2}{105} & \frac{13ml}{420} & 0 & -\frac{ml^2}{140} & 0 \\ & \frac{13m}{35}+m_t & 0 & -\frac{11ml}{210} & 0 \\ & & \frac{13m}{35}+m_t & 0 & -\frac{11ml}{210} \\ & sym & & \frac{ml^2}{105} & 0 \\ & & & & \frac{ml^2}{105} \end{bmatrix}, \tag{25}$$

$$\overline{\mathbf{C}} = 2\mathbf{B}^{\mathbf{T}}(\mathbf{M}+\mathbf{M_t})\dot{\mathbf{B}} = 2\Omega \begin{bmatrix} 0 & 0 & -\frac{13ml}{420} & 0 & \frac{ml^2}{140} \\ 0 & 0 & -\frac{13m}{35}-m_t & 0 & \frac{11ml}{210} \\ \frac{13ml}{420} & \frac{13m}{35}+m_t & 0 & -\frac{11ml}{210} & 0 \\ 0 & 0 & -\frac{11ml}{210} & 0 & -\frac{ml^2}{105} \\ -\frac{ml^2}{140} & -\frac{11ml}{210} & 0 & \frac{ml^2}{105} & 0 \end{bmatrix}. \tag{26}$$

Note that the matrix $\overline{\mathbf{C}}$ is skew-symmetric. Using Eq. 10 and the definition of $\mathbf{K}_l$ given by Eq. A-5 in the appendix of this paper, the stiffness matrix $\overline{\mathbf{K}}$ of Eq. 24 can be written as

$$\overline{\mathbf{K}} = \overline{\mathbf{K}}_l + \overline{\mathbf{K}}_t = \varepsilon_A\overline{\mathbf{K}}_A + \varepsilon_M\overline{\mathbf{K}}_M + \varepsilon_B\overline{\mathbf{K}}_B + \overline{\mathbf{K}}_t, \tag{27}$$

where

$$\overline{\mathbf{K}}_A = \mathbf{B}^{\mathbf{T}}\mathbf{K}_A\mathbf{B} = \frac{EA}{210l}\begin{bmatrix} 12l^2 & 18l & 0 & -2l^2 & 0 \\ & -36 & 0 & -3l & 0 \\ & & -36 & 0 & -3l \\ & sym & & -2l^2 & 0 \\ & & & & -2l^2 \end{bmatrix}, \tag{28}$$

$$\overline{\mathbf{K}}_M = \mathbf{B}^{\mathbf{T}}\mathbf{K}_M\mathbf{B} = \frac{EA}{210l}\begin{bmatrix} 18l^2 & -36l & 0 & -3l^2 & 0 \\ & 324 & 0 & -36l & 0 \\ & & 324 & 0 & -36l \\ & sym & & 18l^2 & 0 \\ & & & & 18l^2 \end{bmatrix}, \tag{29}$$

$$\overline{\mathbf{K}}_B = \mathbf{B}^{\mathbf{T}}\mathbf{K}_B\mathbf{B} = \frac{EA}{210l}\begin{bmatrix} -2l^2 & -3l & 0 & -2l^2 & 0 \\ & -36 & 0 & 18l & 0 \\ & & -36 & 0 & 18l \\ & sym & & 12l^2 & 0 \\ & & & & 12l^2 \end{bmatrix}, \tag{30}$$

$$\overline{\mathbf{K}}_t = \mathbf{B}^{\mathbf{T}}\mathbf{K}_t\mathbf{B} = \frac{EI}{l^3}\begin{bmatrix} 4l^2 & -6l & 0 & 2l^2 & 0 \\ & 12 & 0 & -6l & 0 \\ & & 12 & 0 & -6l \\ & sym & & 4l^2 & 0 \\ & & & & 4l^2 \end{bmatrix}. \tag{31}$$

The matrices $\mathbf{K}_A$, $\mathbf{K}_M$, $\mathbf{K}_B$ and $\mathbf{K}_t$ and the strains ε_A, ε_M and ε_B are defined in the appendix. The vector $\overline{\mathbf{F}}_m$ in the right-hand side of Eq. 24 absorbs the terms depending on $\mathbf{e}_r$, and is defined as

$$\overline{\mathbf{F}}_m = \Omega^2\mathbf{B}^{\mathbf{T}}(\mathbf{M}+\mathbf{M_t})\mathbf{e}_r = \Omega^2 R\begin{bmatrix} \frac{ml}{12} & \frac{m}{2}+m_t & 0 & -\frac{ml}{12} & 0 \end{bmatrix}^{\mathrm{T}}. \tag{32}$$

This vector does not depend of the stiffness matrix since the product $\mathbf{K}\mathbf{e}_r$ is identically equal to zero.

From Eq. 24 it is clear that, for large values of the angular velocity Ω, the matrix $\Omega^2\overline{\mathbf{M}}$ could become the source of the instability, unless the elements of the matrix $\overline{\mathbf{K}}$ also increase. On the other hand, the matrix $\overline{\mathbf{K}}$ is a linear function of the longitudinal strains ε_A, ε_M and ε_B, which play a key role in this problem. It is important to point out that the relationship between ε_A, ε_M and ε_B and the independent coordinates q_i is highly nonlinear (see Eq. A-4 in the appendix). Consequently, the stiffness matrix $\overline{\mathbf{K}}$ is a nonlinear function of the coordinates. The equation of motion (Eq. 24) is a Hill equation. In the following section a solution of this equation that holds in the case of small deformation is obtained.

5 SOLUTION OF THE EQUATION OF MOTION

In this section, Eq. 24 is solved by means of a linearization that holds as long as the deformation remains small. As a result of this linearization, the Hill equation is reduced to a differential equation with constant coefficients, whose solution is expressed as the sum of a constant term $\mathbf{q}_0$ (particular solution) and a time dependent term $\mathbf{q}_\delta$ (complementary function).

Particular Solution Note that the right-hand side of Eq. 24 is constant, and, therefore, we seek a solution of the type $\mathbf{q} = \mathbf{q}_0$ =const., that corresponds to the static equilibrium of the beam in the rotating coordinate system. In this case, Eq. 24 becomes

$$[\overline{\mathbf{K}}(\mathbf{q}_0) - \Omega^2\overline{\mathbf{M}}]\mathbf{q}_0 = \overline{\mathbf{F}}_m. \tag{33}$$

It is convenient to write the vector $\mathbf{q}_0$ as the sum of two vectors,

$$\mathbf{q}_0 = \mathbf{q}_{rb} + \mathbf{q}_{\delta 0}, \tag{34}$$

where $\mathbf{q}_{rb}$ represents the rigid-body (undeformed) configuration of the beam, and $\mathbf{q}_{\delta 0}$ contains the deformation terms. This representation is convenient as the elements of $\mathbf{q}_{\delta 0}$ are very small. In fact, using Eq. A-8 given in the appendix, it is possible to write:

$$\mathbf{q}_{rb} = \begin{bmatrix} 1 & l & 0 & 1 & 0 \end{bmatrix}^{\mathrm{T}}, \quad \mathbf{q}_{\delta 0} = \begin{bmatrix} \varepsilon_{A0} & l\varepsilon_{M0} & 0 & \varepsilon_{B0} & 0 \end{bmatrix}^{\mathrm{T}}, \tag{35}$$

where the subscript 0 means that the quantities are not time dependent.

The equation that governs the static equilibrium in the rotating coordinate system can then be written as

$$\overline{\mathbf{K}}(\mathbf{q}_{rb} + \mathbf{q}_{\delta 0}) = \Omega^2\overline{\mathbf{M}}(\mathbf{q}_{rb} + \mathbf{q}_{\delta 0}) + \overline{\mathbf{F}}_m. \tag{36}$$

In this equation, for the stated assumptions, the vector $\mathbf{q}_{\delta 0}$ is negligible with respect to the vector $\mathbf{q}_{rb}$. Furthermore, it is possible to show that the following equation holds:

$$\overline{\mathbf{K}}\mathbf{q}_{rb} = \overline{\mathbf{K}}_{\delta 0}\mathbf{q}_{\delta 0}, \tag{37}$$

where

$$\overline{\mathbf{K}}_{\delta 0} = \left[\begin{array}{cccccc} \overline{\mathbf{K}}_A \mathbf{q}_{rb} & \frac{1}{l}\overline{\mathbf{K}}_M \mathbf{q}_{rb} & \mathbf{0} & \overline{\mathbf{K}}_B \mathbf{q}_{rb} & \mathbf{0} \end{array} \right]^{\mathrm{T}}. \tag{38}$$

This matrix is constant and can be explicitly written as

$$\overline{\mathbf{K}}_{\delta 0} = \frac{EA}{30l} \left[\begin{array}{ccccc} 4l^2 & -3l & 0 & -2l^2 & 0 \\ & 36 & 0 & -3l & 0 \\ & & 0 & 0 & 0 \\ & sym & & 4l^2 & 0 \\ & & & & 0 \end{array} \right]. \tag{39}$$

The final equation simply becomes

$$\overline{\mathbf{K}}_{\delta 0} \mathbf{q}_{\delta 0} = \Omega^2 \overline{\mathbf{M}} \mathbf{q}_{rb} + \overline{\mathbf{F}}_m. \tag{40}$$

This equation leads to a solution $\mathbf{q}_{\delta 0}$ from which it is possible to calculate the corresponding strains ε_{A0}, ε_{M0} and ε_{B0} as

$$\varepsilon_{A0} = \frac{m\Omega^2}{EA}\frac{2R+l}{2} + \frac{m_t\Omega^2}{EA}(R+l), \tag{41}$$

$$\varepsilon_{M0} = \frac{m\Omega^2}{EA}\frac{3R+2l}{6} + \frac{m_t\Omega^2}{EA}(R+l), \tag{42}$$

$$\varepsilon_{B0} = \frac{m_t\Omega^2}{EA}(R+l). \tag{43}$$

These values correspond to the exact analytical solution, according to which the strain distribution is parabolic, and it has a maximum at the left end, as shown in Fig. 10. This result is a good test for the force model introduced in Section 2, as for this small deformation problem the solution is equal to the correct analytical solution.

General Solution The result of the previous analysis can be conveniently reported as

$$\mathbf{q}_0 = \left[\begin{array}{ccccc} \varepsilon_{A0}+1 & l(\varepsilon_{M0}+1) & 0 & \varepsilon_{B0}+1 & 0 \end{array} \right]^{\mathrm{T}}, \tag{44}$$

where the strains ε_{A0}, ε_{M0} and ε_{B0} are given by Eqs. 41-43. Then, the complete solution defined by the vector $\mathbf{q}$ can be written as

$$\mathbf{q} = \mathbf{q}_0 + \mathbf{q}_\delta, \tag{45}$$

where $\mathbf{q}_0$ is constant, while $\mathbf{q}_\delta = \begin{bmatrix} q_{1\delta} & q_{2\delta} & q_{3\delta} & q_{4\delta} & q_{5\delta} \end{bmatrix}^{\mathrm{T}}$ contains the small dynamic terms. A similar decomposition applies for the strains ε_A, ε_M and ε_B, and consequently for the matrix $\overline{\mathbf{K}}$ as well. It is possible to show that, under the assumption of small deformations, the following relationships hold:

$$\varepsilon_A = \varepsilon_{A0} + \varepsilon_{A\delta}, \quad \varepsilon_{A\delta} = q_{1\delta}, \tag{46}$$

$$\varepsilon_M = \varepsilon_{M0} + \varepsilon_{M\delta}, \quad \varepsilon_{M\delta} = q_{2\delta}/l, \tag{47}$$

$$\varepsilon_B = \varepsilon_{B0} + \varepsilon_{B\delta}, \quad \varepsilon_{B\delta} = q_{4\delta}, \tag{48}$$

and the matrix $\overline{\mathbf{K}}$ becomes

$$\overline{\mathbf{K}} = \overline{\mathbf{K}}_0 + \overline{\mathbf{K}}_\delta, \tag{49}$$

where $\overline{\mathbf{K}}_0$ is the matrix that is obtained from Eq. 27 using ε_{A0}, ε_{M0} and ε_{B0}, and $\overline{\mathbf{K}}_\delta$ is the matrix obtained using $\varepsilon_{A\delta}$, $\varepsilon_{M\delta}$ and $\varepsilon_{B\delta}$.

With these substitutions, the equation of motion (Eq. 24) becomes

$$\overline{\mathbf{M}}\ddot{\mathbf{q}}_\delta + \overline{\mathbf{C}}\dot{\mathbf{q}}_\delta + (\overline{\mathbf{K}}_0 - \Omega^2\overline{\mathbf{M}})\mathbf{q}_0 + \overline{\mathbf{K}}_\delta\mathbf{q}_0 + (\overline{\mathbf{K}}_0 - \Omega^2\overline{\mathbf{M}})\mathbf{q}_\delta + \overline{\mathbf{K}}_\delta\mathbf{q}_\delta = \overline{\mathbf{F}}_m, \tag{50}$$

which, after eliminating the static solution and the second order term $\overline{\mathbf{K}}_\delta\mathbf{q}_\delta$, yields

$$\overline{\mathbf{M}}\ddot{\mathbf{q}}_\delta + \overline{\mathbf{C}}\dot{\mathbf{q}}_\delta + \overline{\mathbf{K}}_\delta\mathbf{q}_0 + (\overline{\mathbf{K}}_0 - \Omega^2\overline{\mathbf{M}})\mathbf{q}_\delta = \mathbf{0}. \tag{51}$$

It can be shown that the product $\overline{\mathbf{K}}_\delta\mathbf{q}_0$ can be written as follows:

$$\overline{\mathbf{K}}_\delta\mathbf{q}_0 = \overline{\mathbf{K}}_{\delta 0}\mathbf{q}_\delta, \tag{52}$$

where the matrix $\overline{\mathbf{K}}_{\delta 0}$ is defined by Eq. 38. After substitutions, the final form of the equation of motion is given by

$$\overline{\mathbf{M}}\ddot{\mathbf{q}}_\delta + \overline{\mathbf{C}}\dot{\mathbf{q}}_\delta + \overline{\mathbf{K}}_{eq}\mathbf{q}_\delta = \mathbf{0}, \tag{53}$$

where the equivalent stiffness matrix $\overline{\mathbf{K}}_{eq}$ is defined as

$$\overline{\mathbf{K}}_{eq} = \overline{\mathbf{K}}_0 + \overline{\mathbf{K}}_{\delta 0} - \Omega^2\overline{\mathbf{M}}. \tag{54}$$

Note that the stiffness matrix $\overline{\mathbf{K}}_{eq}$ is constant as a result of using variables defined in the rotating coordinate system and as a result of the linearization assumption.

A solution for Eq. 53 of the type

$$\mathbf{q}_\delta = \mathbf{Q}_\delta e^{\lambda t} \tag{55}$$

results in five complex eigenvalues $\lambda_i = \alpha_i + j\omega_i$. When the real part α_i of λ_i is not positive, the solution does not show any instability. In the next section, numerical results will be provided for different values of the angular velocity Ω and different combinations of hub radius R and tip mass m_t. However, in the remainder of this section, it is shown that for any value of the speed of rotation Ω, the system remains stable. Consequently, the only limit on Ω is given by the strength of the material and/or the maximum admissible deformation.

Substituting the values of ε_{A0}, ε_{M0} and ε_{B0} obtained with the static analysis, Eqs. 41-43, in the expression of the matrix $\overline{\mathbf{K}}_0$, one obtains the equivalent stiffness matrix

$$\overline{\mathbf{K}}_{eq} = \overline{\mathbf{K}}_t + \overline{\mathbf{K}}_{\delta 0} + \Omega^2(\overline{\mathbf{K}}_{ml} + \overline{\mathbf{K}}_{mR} + \overline{\mathbf{K}}_{m_t l} + \overline{\mathbf{K}}_{m_t R}), \tag{56}$$

where the matrices $\overline{\mathbf{K}}_{ml}$, $\overline{\mathbf{K}}_{mR}$, $\overline{\mathbf{K}}_{m_t l}$, and $\overline{\mathbf{K}}_{m_t R}$ are defined as

$$\overline{\mathbf{K}}_{ml} = \frac{m}{420}\begin{bmatrix} 20l^2 & -19l & 0 & -l^2 & 0 \\ & 24 & 0 & -5l & 0 \\ & & 24 & 0 & -5l \\ & sym & & 6l^2 & 0 \\ & & & & 6l^2 \end{bmatrix}, \tag{57}$$

$$\overline{\mathbf{K}}_{mR} = \frac{mR}{420l}\begin{bmatrix} 42l^2 & 0 & 0 & -7l^2 & 0 \\ & 252 & 0 & -42l & 0 \\ & & 252 & 0 & -42l \\ & sym & & 14l^2 & 0 \\ & & & & 14l^2 \end{bmatrix}, \tag{58}$$

$$\overline{\mathbf{K}}_{m_t l} = \frac{m_t}{420}\begin{bmatrix} 56l^2 & -42l & 0 & -14l^2 & 0 \\ & 84 & 0 & -42l & 0 \\ & & 84 & 0 & -42l \\ & sym & & 56l^2 & 0 \\ & & & & 56l^2 \end{bmatrix}, \tag{59}$$

$$\overline{\mathbf{K}}_{m_t R} = \frac{m_t R}{420l}\begin{bmatrix} 56l^2 & -42l & 0 & -14l^2 & 0 \\ & 504 & 0 & -42l & 0 \\ & & 504 & 0 & -42l \\ & sym & & 56l^2 & 0 \\ & & & & 56l^2 \end{bmatrix}. \tag{60}$$

Equation 56 shows how $\overline{\mathbf{K}}_{eq}$ can be decomposed into the sum of several matrices that are either positive definite or positive semi-definite. Consequently, the matrix $\overline{\mathbf{K}}_{eq}$ is always a positive definite matrix, despite the presence of the term $-\Omega^2\overline{\mathbf{M}}$ in Eq. 54. This demonstrates that, for any given value of the angular velocity Ω, the nonlinear stiffness matrix includes stiffening effects, as $\overline{\mathbf{K}}_0$ increases with Ω^2.

From this result, it is possible to define a Liapunov function [10] V as

$$V = \frac{1}{2}\dot{\mathbf{q}}_\delta^{\mathrm{T}}\overline{\mathbf{M}}\dot{\mathbf{q}}_\delta + \frac{1}{2}\mathbf{q}_\delta^{\mathrm{T}}\overline{\mathbf{K}}_{eq}\mathbf{q}_\delta. \tag{61}$$

This function is positive definite for all $\mathbf{q}_\delta \neq \mathbf{0}$ and $\dot{\mathbf{q}}_\delta \neq \mathbf{0}$. It is easy to show that the time derivative of V is always equal to zero. Since $\overline{\mathbf{K}}_{eq}$ is symmetric and $\overline{\mathbf{C}}$ is skew-symmetric, so that $\dot{\mathbf{q}}_\delta^{\mathrm{T}}\overline{\mathbf{C}}\dot{\mathbf{q}}_\delta = 0$ for all $\dot{\mathbf{q}}_\delta$, then

$$\begin{aligned} \dot{V} &= \dot{\mathbf{q}}_\delta^{\mathrm{T}}\overline{\mathbf{M}}\ddot{\mathbf{q}}_\delta + \mathbf{q}_\delta^{\mathrm{T}}\overline{\mathbf{K}}_{eq}\dot{\mathbf{q}}_\delta \\ &= -\dot{\mathbf{q}}_\delta^{\mathrm{T}}\overline{\mathbf{C}}\dot{\mathbf{q}}_\delta - \dot{\mathbf{q}}_\delta^{\mathrm{T}}\overline{\mathbf{K}}_{eq}\mathbf{q}_\delta + \mathbf{q}_\delta^{\mathrm{T}}\overline{\mathbf{K}}_{eq}\dot{\mathbf{q}}_\delta = 0. \end{aligned}$$

The fact that the Liapunov function is constant implies that any increase in the velocities $|\dot{\mathbf{q}}_\delta|$ is balanced by a decrease in the value of the coordinates $|\mathbf{q}_\delta|$, and vice-versa. Hence, the motion is oscillatory and V is called a *weak Liapunov function* for the system, as the

particular solution is stable but not asymptotically stable. The skew-symmetric matrix $\overline{\mathbf{C}}$ neither introduces nor dissipates any energy in the system.

6 REMARKS ON THE COUPLING BETWEEN AXIAL AND BENDING DEFORMATIONS

It is important to point out that the stiffness matrix $\overline{\mathbf{K}}_{eq}$ defined by Eq. 54 is constant as a result of linearization of the equations of motion which have been obtained using a nonlinear strain-displacement relationship. This is a key step in the development, since an early linearization of the strain-displacement relationship would not be sufficient to represent the stiffening effect. Both models, Model 0 and Model A, are based on the expression of the strain energy given by Eq. 9. The key difference is in the way the longitudinal strain ε_l is measured. Model 0 employs a local element coordinate system in which a longitudinal displacement u_l is measured; then the longitudinal strain is defined as [16]:

$$\varepsilon_l = \frac{\partial u_l}{\partial x}, \tag{62}$$

where x is a coordinate along the axis tangent to the beam centerline. In Model A there is no need to introduce a local coordinate system, since the longitudinal strain is defined as

$$\varepsilon_l = \frac{1}{2}(f^2 - 1). \tag{63}$$

Here f is the deformation gradient for longitudinal deformations [2], and its value depends on longitudinal displacements as well as transverse displacements. A development based on Eq. 63 would result in a nonlinear stiffness matrix even when local element coordinates are used. In this paper, in order to obtain a constant stiffness matrix, the assumption is made that the time dependent term $\mathbf{q}_\delta$ introduced in Section 5 is small as compared to the constant term $\mathbf{q}_0$, so that the effect of $\mathbf{q}_\delta$ on the stiffness matrix becomes negligible. This assumption, however, does not affect the coupling between the longitudinal and transverse

displacements, which does not exist when Model 0 is used [1]. Therefore, in Model A, the bending deformation of the beam depends on the longitudinal displacements when either a fixed or an element frame is used to define the element coordinates.

7 NUMERICAL RESULTS

In this section, the mathematical model presented in the previous section will be used to determine the natural frequencies and mode shapes of the system shown in Fig. 8. The system consists of a beam attached to a rigid hub with a mass attached to the other end. While in the previous section the analysis was made using only one element, the results presented in this section are obtained using ten elements. Hence, the equation that governs the vibrations of the beam is similar to Eq. 53, with the exception that it is generalized for the case of an arbitrary number of finite elements. All the results are presented in a non-dimensional form. Given the parameter

$$\omega_0 = \sqrt{\frac{EI}{ml^3}}, \tag{64}$$

which has the units of an angular velocity, the natural frequencies ω_i are expressed with the ratio ω_i/ω_0, while the speed of rotation Ω is expressed using the ratio

$$\gamma = \Omega/\omega_0. \tag{65}$$

It is possible to check the results obtained when the beam is not rotating, since the analytical solution for this problem exists in the literature [15]. Table 2 shows the natural frequencies of the beam for the first three transverse modes and for the first longitudinal mode for different values of the tip mass. These values are presented using the non-dimensional parameter

$$N = m_t/m, \tag{66}$$

where m is the mass of the beam and m_t is the tip mass. It is clear that there is a good agreement between the exact values of the natural frequencies and the values obtained using the computer simulations.

Tables 3, 4 and 5 present the values of the natural frequencies for the 1st, 2nd and 3rd bending mode respectively, for different values of the non-dimensional angular velocity γ, the ratio R/L and the tip mass ratio N. The results presented are in very good agreement with the results previously obtained by different authors [12, 24]. It is interesting to see that resonance conditions may take place. For the first bending mode with $N = 0$ and $R/L = 0$, the angular velocity equals the natural frequency when $\gamma = 3.88$, the same result as predicted by Yoo et al [24].

Figures 11 and 12 show the change in the mode shapes for different values of the speed of rotation of the beam. The results of Fig. 11 are obtained with $R = 0$ and $m_t = 0$, while in Fig. 12 $R = 2l$ and $m_t = 3m$. These mode shapes are obtained using the dynamic part of the displacements ($\mathbf{q}_\delta$ of Eq. 45); note that for the assumption of small deformations of the beam, the horizontal displacement is not large in the local coordinate system $\eta_1 A \eta_2$. In fact, $\gamma = 50$ corresponds to a very large value of the angular velocity, and in the case of a very flexible beam large deformations are expected.

Finally, Figs 13 and 14 confirm that for small values of the angular velocity a linear approximation applies for the square of the natural frequency. The relationship is of the type

$$\omega^2 = \omega_0^2 + \phi\Omega^2, \tag{67}$$

where ω is the natural frequency when the angular velocity equals Ω, while ω_0 is the natural frequency when the angular velocity is equal to zero; ϕ is called Southwell coefficient. The results obtained with the absolute nodal coordinate formulation are in very good agreement with the values of the Southwell coefficients proposed by Schilhansl [13], who found the

following relationships for the first two bending frequencies:

$$\phi_1 = 0.173 + 1.558 \cdot R/L, \tag{68}$$

$$\phi_2 = 5.380 + 8.631 \cdot R/L. \tag{69}$$

The approximated results presented in Figs. 13 and 14 have been obtained using these expressions for the Southwell coefficients.

8 SUMMARY AND CONCLUSIONS

It is demonstrated in this paper that the effect of the geometric centrifugal stiffening can be automatically accounted for in the finite element absolute nodal coordinate formulation. A continuum mechanics approach is used to obtain the nonlinear expression for the elastic forces that include coupling between the bending and the axial displacements of the rotating beam. Using the absolute nodal coordinate formulation and the proposed elastic force model, a Hill-type equation is obtained. This equation governs the dynamics of the rotating beam subjected to prescribed angular velocity. With the aid of some linearization assumptions, the Hill equation is simplified, and a complete solution is obtained. It is shown analytically that the resulting solution does not exhibit any instability as the angular velocity of the beam increases. The results obtained in this investigation are compared with previously published work. This comparative study shows a very good and consistent agreement between the finite element solution obtained in this study and the solution previously reported by other authors.

APPENDIX

The matrices $\mathbf{M}$ and $\mathbf{M}_t$ that appear in Eq. 15 are defined as follows [16]:

$$\mathbf{M} = m \begin{bmatrix} \frac{13}{35} & 0 & \frac{11l}{210} & 0 & \frac{9}{70} & 0 & \frac{-13l}{420} & 0 \\ & \frac{13}{35} & 0 & \frac{11l}{210} & 0 & \frac{9}{70} & 0 & \frac{-13l}{420} \\ & & \frac{l^2}{105} & 0 & \frac{13l}{420} & 0 & \frac{-l^2}{140} & 0 \\ & & & \frac{l^2}{105} & 0 & \frac{13l}{420} & 0 & \frac{-l^2}{140} \\ & & & & \frac{13}{35} & 0 & \frac{-11l}{210} & 0 \\ & & & & & \frac{13}{35} & 0 & \frac{-11l}{210} \\ & & sym & & & & \frac{l^2}{105} & 0 \\ & & & & & & & \frac{l^2}{105} \end{bmatrix}, \tag{A-1}$$

$$\mathbf{M}_t = m_t \begin{bmatrix} 0 & 0 & 0 & 0 & 0 & 0 & 0 & 0 \\ & 0 & 0 & 0 & 0 & 0 & 0 & 0 \\ & & 0 & 0 & 0 & 0 & 0 & 0 \\ & & & 0 & 0 & 0 & 0 & 0 \\ & & & & 1 & 0 & 0 & 0 \\ & & & & & 1 & 0 & 0 \\ & & sym & & & & 0 & 0 \\ & & & & & & & 0 \end{bmatrix}, \tag{A-2}$$

where m is the mass of the beam element and l is its length; m_t is the tip mass.

The expression of the elastic forces is obtained using Model III presented in Ref. 2. This model, which is referred to as Model A in this paper, holds in the case of small deformations. The matrix $\mathbf{K}_l$ of Eq. 10 is written as sum of three matrices that depend on the three quantities ε_A, ε_M and ε_B defined in general as

$$\varepsilon_A = \sqrt{e_3^2 + e_4^2} - 1, \quad \varepsilon_M = \frac{1}{l}\sqrt{(e_5 - e_1)^2 + (e_6 - e_2)^2} - 1, \quad \varepsilon_B = \sqrt{e_7^2 + e_8^2} - 1. \tag{A-3}$$

Using the relationship between the coordinates e_i and q_i as given by Eq. 20, one obtains

$$\varepsilon_A = |q_1| - 1, \quad \varepsilon_M = \frac{1}{l}\sqrt{q_2^2 + q_3^2} - 1, \quad \varepsilon_B = \sqrt{q_4^2 + q_5^2} - 1. \tag{A-4}$$

The terms ε_A and ε_B physically represent the longitudinal strains at A and B respectively; and ε_M represents the average longitudinal strain along the element length. Using these three quantities, the stiffness matrix $\mathbf{K}_l$ can be written as

$$\mathbf{K}_l = \varepsilon_A \mathbf{K}_A + \varepsilon_M \mathbf{K}_M + \varepsilon_B \mathbf{K}_B, \tag{A-5}$$

where

$$\mathbf{K}_A = \frac{EA}{l}\begin{bmatrix} \frac{-6}{35} & 0 & \frac{-6l}{70} & 0 & \frac{6}{35} & 0 & \frac{l}{70} & 0 \\ & \frac{-6}{35} & 0 & \frac{-6l}{70} & 0 & \frac{6}{35} & 0 & \frac{l}{70} \\ & & \frac{6l^2}{105} & 0 & \frac{6l}{70} & 0 & \frac{-l^2}{105} & 0 \\ & & & \frac{6l^2}{105} & 0 & \frac{6l}{70} & 0 & \frac{-l^2}{105} \\ & & & & \frac{-6}{35} & 0 & \frac{-l}{70} & 0 \\ & sym & & & & \frac{-6}{35} & 0 & \frac{-l}{70} \\ & & & & & & \frac{-l^2}{105} & 0 \\ & & & & & & & \frac{-l^2}{105} \end{bmatrix}, \tag{A-6}$$

$$\mathbf{K}_M = \frac{EA}{l}\begin{bmatrix} \frac{54}{35} & 0 & \frac{12l}{70} & 0 & \frac{-54}{35} & 0 & \frac{12l}{70} & 0 \\ & \frac{54}{35} & 0 & \frac{12l}{70} & 0 & \frac{-54}{35} & 0 & \frac{12l}{70} \\ & & \frac{9l^2}{105} & 0 & \frac{-12l}{70} & 0 & \frac{-l^2}{70} & 0 \\ & & & \frac{9l^2}{105} & 0 & \frac{-12l}{70} & 0 & \frac{-l^2}{70} \\ & & & & \frac{54}{35} & 0 & \frac{-12l}{70} & 0 \\ & sym & & & & \frac{54}{35} & 0 & \frac{-12l}{70} \\ & & & & & & \frac{9l^2}{105} & 0 \\ & & & & & & & \frac{9l^2}{105} \end{bmatrix}, \tag{A-7}$$

$$\mathbf{K}_B = \frac{EA}{l}\begin{bmatrix} \frac{-6}{35} & 0 & \frac{l}{70} & 0 & \frac{6}{35} & 0 & \frac{-6l}{70} & 0 \\ & \frac{-6}{35} & 0 & \frac{l}{70} & 0 & \frac{6}{35} & 0 & \frac{-6l}{70} \\ & & \frac{-l^2}{105} & 0 & \frac{-l}{70} & 0 & \frac{-l^2}{105} & 0 \\ & & & \frac{-l^2}{105} & 0 & \frac{-l}{70} & 0 & \frac{-l^2}{105} \\ & & & & \frac{-6}{35} & 0 & \frac{6l}{70} & 0 \\ & sym & & & & \frac{-6}{35} & 0 & \frac{6l}{70} \\ & & & & & & \frac{6l^2}{105} & 0 \\ & & & & & & & \frac{6l^2}{105} \end{bmatrix}. \tag{A-8}$$

In the case of small deformations, the relationships in Eq. A-4 can be simplified, since $q_1 \approx q_4 \approx 1$, $q_2 \approx l$, and $q_3 \approx q_5 \approx 0$. As a result, the following linear relationships can be obtained:

$$\varepsilon_A = q_1 - 1, \quad \varepsilon_M = q_2/l - 1, \quad \varepsilon_B = q_4 - 1. \tag{A-9}$$

The stiffness matrix $\mathbf{K}_t$ of Eq. 10 is constant and is defined as

$$\mathbf{K}_t = \frac{EI}{l^3}\begin{bmatrix} 12 & 0 & 6l & 0 & -12 & 0 & 6l & 0 \\ & 12 & 0 & 6l & 0 & -12 & 0 & 6l \\ & & 4l^2 & 0 & -6l & 0 & 2l^2 & 0 \\ & & & 4l^2 & 0 & -6l & 0 & 2l^2 \\ & & & & 12 & 0 & -6l & 0 \\ & sym & & & & 12 & 0 & -6l \\ & & & & & & 4l^2 & 0 \\ & & & & & & & 4l^2 \end{bmatrix}. \tag{A-10}$$

Acknowledgment

This research was supported by the U.S. Army Research Office, Research Triangle Park, NC, and, in part, by the National Science Foundation.

REFERENCES

[1] M. Berzeri, M. Campanelli and A.A. Shabana *Multibody System Dynamics*, in print. Definition of the Elastic Forces in the Finite Element Absolute Nodal Coordinate Formulation and the Floating Frame of Reference Formulation.

[2] M. Berzeri and A.A. Shabana *Journal of Sound and Vibration*, submitted for publication. Developments of Simple Models for the Elastic Forces in the Absolute Nodal Coordinate Formulation.

[3] Z.-E. Boutaghou and A.G. Erdman 1993 *Journal of Sound and Vibration* **164**(2), 207-223. On various non-linear rod theories for the dynamic analysis of multi-body systems, Part I: Formulations.

[4] Z.-E. Boutaghou and A.G. Erdman 1993 *Journal of Sound and Vibration* **164**(2), 225-236. On various non-linear rod theories for the dynamic analysis of multi-body systems, Part II: Applications.

[5] M. Campanelli, M. Berzeri and A. A. Shabana 1999 *Technical Report No. MBS99-2-UIC*, University of Illinois at Chicago. Comparison between the absolute nodal coordinate formulation and incremental procedures.

[6] H. El-Absy and A. A. Shabana 1997 *Journal of Sound and Vibration* **207**(4), 465-496. Geometric stiffness and stability of rigid body modes.

[7] J. L. Escalona, H. A. Hussien and A. A. Shabana 1998 *Journal of Sound and Vibration* **214**(5), 833-851. Application of the absolute nodal coordinate formulation to multibody system dynamics.

[8] E.H.K. Fung and Z.X. Shi 1997 *Journal of Sound and Vibration* **202**(2), 259-269. Vibration frequencies of a constrained flexible arm carrying an end mass.

[9] E.H.K. Fung and D.T.W. Yau 1999 *Journal of Sound and Vibration* **224**(5), 809-841. Effect of centrifugal stiffening on the vibration frequencies of a constrained flexible arm.

[10] D.W. Jordan and P. Smith 1987 *Nonlinear Ordinary Differential Equations.* Oxford University Press, New York; 2nd edition.

[11] T.R. Kane, R.R. Ryan and A.K. Banerjee 1987 *AIAA Journal of Guidance, Control, and Dynamics* **10**(2), 139-151. Dynamics of a cantilever beam attached to a moving base.

[12] S. Putter and H. Manor 1978 *Journal of Sound and Vibration* **56**(2), 175-185. Natural frequencies of radial rotating beams.

[13] M.J. Schilhansl 1958 *Journal of Applied Mechanics* **25**, 28-30. Bending frequency of a rotating cantilever beam.

[14] R. Schwertassek and O. Wallrapp 1999 *Dynamik flexibler Mehrkorpersysteme.* Vieweg.

[15] A.A. Shabana 1991 *Theory of Vibration.* Vol. II. Springer-Verlag.

[16] A.A. Shabana 1998 *Dynamics of Multibody Systems.* Cambridge University Press; 2nd edition.

[17] A.A. Shabana and R. Schwertassek 1998 *Int. Journal of Non-Linear Mechanics* **33**(3), 417-432. Equivalence of the floating frame of reference approach and finite element formulations.

[18] J.C. Simo and L. Vu-Quoc 1987 *Journal of Sound and Vibration* **119**(3), 487-508. The role of non-linear theories in transient dynamic analysis of flexible structures.

[19] O. Wallrapp and R. Schwertassek 1991 *Int. Journal for Numerical Methods in Engineering* **32**, 1833-1850. Representation of geometric stiffening in multibody system simulation.

[20] A.D. Wright, C.E. Smith, R.W. Thresher and J.L.C. Wang 1982 *Journal of Applied Mechanics* **49**, 197-202. Vibration modes of centrifugally stiffened beams.

[21] S.-C. Wu and E.J. Haug 1988 *Int. Journal for Numerical Methods in Engineering* **26**, 2211-2226. Geometric non-linear substructuring for dynamics of flexible mechanical systems.

[22] R.Y. Yakoub and A.A. Shabana 1999 *DETC99-ASME Design Eng. Technical Conferences*, Paper no. VIB-8204. A numerical approach to solving flexible multibody systems using the absolute nodal coordinate formulation.

[23] A. Yigit, R.A. Scott and A. Galip Ulsoy 1988 *Journal of Sound and Vibration* **121**(2), 201-210. Flexural motion of a radially rotating beam attached to a rigid body.

[24] H.H. Yoo and S.H. Shin 1998 *Journal of Sound and Vibration* **212**(5), 807-828. Vibration analysis of rotating cantilever beams.

Table 1. Geometric and inertia properties of the beams used in Refs. 19 and 21

Description	Symbol	Ref. 19	Ref. 21
Length (m)	L	1.000E+01	8.000E+00
Mass density (kg/m^3)	ρ	3.000E+03	2.767E+03
Cross sectional area (m^2)	A	4.000E-04	7.299E-05
Second moment of area (m^4)	I	1.997E-07	8.214E-09
Mass (kg)	m	1.200E+01	1.615E+00
Modulus of elasticity (Pa)	E	7.000E+10	6.895E+10
Bending stiffness (N•m^2)	EI	1.398E+04	5.664E+02
Moment of inertia about one end (kg•m^2)	J	4.000E+02	3.446E+01

Table 2. Non-dimensional frequencies(*) for the first three transverse modes and the first longitudinal mode using different end masses N.

		Non-dimensional Frequencies ω/ω_0	
N	**MODE**	**Exact value**	**Simulation**
0	TRANSV-I	3.5160	3.5160
	TRANSV-II	22.0345	22.0352
	TRANSV-III	61.6972	61.7129
	LONGIT-I	339.6316	339.6347
1	TRANSV-I	1.5573	1.5573
	TRANSV-II	16.2501	16.2504
	TRANSV-III	50.8958	50.9046
	LONGIT-I	186.0181	186.0152
2	TRANSV-I	1.1582	1.1582
	TRANSV-II	15.8609	15.8612
	TRANSV-III	50.4476	50.4563
	LONGIT-I	141.2478	141.2455
3	TRANSV-I	0.9628	0.9628
	TRANSV-II	15.7198	15.7200
	TRANSV-III	50.2907	50.2993
	LONGIT-I	118.3049	118.3030
4	TRANSV-I	0.8415	0.8415
	TRANSV-II	15.6469	15.6471
	TRANSV-III	50.2108	50.2194
	LONGIT-I	103.8042	103.8024

(*)Results obtained using the absolute nodal coordinate formulation and 10 elements

Table 3. Non-dimensional frequencies(*) for the first transverse mode using different end masses N and different values for the ratio R/L

		First Transverse Mode: Non-dimensional Frequencies							
N	R/L	γ=1	γ=2	γ=3	γ=4	γ=5	γ=10	γ=20	γ=50
0	0	3.543	3.622	3.743	3.897	4.072	5.041	6.739	10.278
	1	3.758	4.400	5.290	6.313	7.409	13.237	25.136	59.467
	2	3.961	5.059	6.471	8.023	9.639	17.996	34.840	83.416
	3	4.154	5.639	7.464	9.421	11.433	21.722	42.360	101.933
	4	4.338	6.164	8.337	10.632	12.976	24.888	48.726	117.619
	5	4.515	6.647	9.125	11.715	14.350	27.690	54.347	131.491
1	0	1.617	1.768	1.957	2.152	2.340	3.141	4.308	6.615
	1	1.967	2.832	3.822	4.847	5.884	11.094	21.280	48.114
	2	2.262	3.585	5.025	6.493	7.970	15.353	29.773	68.198
	3	2.521	4.201	5.985	7.792	9.606	18.658	36.333	83.911
	4	2.754	4.735	6.807	8.899	10.997	21.455	41.880	97.342
	5	2.969	5.211	7.538	9.880	12.227	23.926	46.777	109.304
2	0	1.236	1.411	1.605	1.791	1.963	2.665	3.662	5.611
	1	1.655	2.581	3.580	4.596	5.616	10.686	20.394	44.529
	2	1.984	3.355	4.789	6.234	7.681	14.861	28.619	63.710
	3	2.263	3.977	5.742	7.517	9.291	18.093	34.972	78.913
	4	2.510	4.510	6.555	8.607	10.658	20.827	40.349	92.011
	5	2.734	4.985	7.275	9.571	11.865	23.240	45.100	103.733
3	0	1.053	1.239	1.429	1.605	1.765	2.407	3.310	5.063
	1	1.516	2.467	3.468	4.478	5.488	10.480	19.867	42.365
	2	1.863	3.251	4.679	6.112	7.544	14.613	27.932	61.145
	3	2.152	3.875	5.630	7.388	9.144	17.809	34.170	76.177
	4	2.404	4.408	6.439	8.471	10.499	20.511	39.456	89.192
	5	2.631	4.881	7.154	9.428	11.697	22.896	44.132	100.870
4	0	0.942	1.132	1.317	1.485	1.636	2.236	3.076	4.699
	1	1.435	2.400	3.401	4.406	5.409	10.343	19.471	40.862
	2	1.793	3.190	4.613	6.039	7.461	14.448	27.420	59.436
	3	2.087	3.814	5.562	7.311	9.054	17.619	33.578	74.409
	4	2.343	4.347	6.369	8.389	10.403	20.301	38.805	87.412
	5	2.572	4.819	7.082	9.342	11.594	22.667	43.434	99.094

(*)Results obtained using the absolute nodal coordinate formulation and 10 elements

Table 4. Non-dimensional frequencies(*) for the second transverse mode using different end masses N and different values for the ratio R/L

		Second Transverse Mode: Non-dimensional Frequencies							
N	R/L	γ=1	γ=2	γ=3	γ=4	γ=5	γ=10	γ=20	γ=50
0	0	22.159	22.527	23.127	23.941	24.949	32.113	51.318	115.751
	1	22.353	23.281	24.747	26.659	28.923	43.221	76.560	181.268
	2	22.546	24.010	26.261	29.107	32.380	51.842	94.995	228.201
	3	22.736	24.716	27.687	31.351	35.476	59.134	110.274	266.872
	4	22.925	25.401	29.038	33.433	38.304	65.570	123.620	300.537
	5	23.113	26.067	30.324	35.384	40.922	71.394	135.627	330.731
1	0	16.727	18.081	20.128	22.672	25.555	42.275	78.611	189.220
	1	17.261	19.979	23.809	28.281	33.119	59.352	114.031	278.927
	2	17.777	21.708	26.978	32.918	39.206	72.428	140.718	345.992
	3	18.279	23.305	29.800	36.958	44.441	83.442	163.061	402.092
	4	18.768	24.796	32.367	40.584	49.102	93.140	182.661	451.324
	5	19.243	26.199	34.739	43.901	53.345	101.905	200.122	495.732
2	0	16.695	18.968	22.220	26.062	30.252	53.190	101.246	246.177
	1	17.556	21.834	27.459	33.721	40.300	74.777	145.317	357.142
	2	18.375	24.350	31.811	39.879	48.227	91.302	178.833	441.165
	3	19.157	26.619	35.612	45.172	54.984	105.220	206.931	511.684
	4	19.907	28.701	39.028	49.885	60.972	117.478	231.638	573.680
	5	20.629	30.635	42.155	54.175	66.406	128.557	253.947	629.659
3	0	16.903	20.015	24.284	29.169	34.384	62.200	119.638	292.310
	1	18.071	23.703	30.777	38.449	46.398	87.470	170.978	421.272
	2	19.164	26.865	36.066	45.811	55.794	106.821	210.057	519.360
	3	20.195	29.674	40.641	52.102	63.774	122.896	242.910	601.812
	4	21.173	32.226	44.728	57.686	70.834	137.494	271.815	674.352
	5	22.106	34.580	48.457	62.757	77.233	150.478	297.926	739.879
4	0	17.172	21.058	26.214	31.986	38.067	70.028	135.548	332.164
	1	18.628	25.467	33.776	42.643	51.758	98.497	193.198	476.944
	2	19.974	29.182	39.862	51.034	62.416	120.315	237.177	587.331
	3	21.229	32.451	45.096	58.181	71.452	138.697	274.176	680.196
	4	22.410	35.403	49.757	64.513	79.438	154.892	306.741	761.927
	5	23.529	38.115	54.000	70.258	86.673	169.535	336.165	835.769

(*)Results obtained using the absolute nodal coordinate formulation and 10 elements

Table 5. Non-dimensional frequencies(*) for the third transverse mode using different end masses N and different values for the ratio R/L

		Third Transverse Mode: Non-dimensional Frequencies							
N	R/L	γ=1	γ=2	γ=3	γ=4	γ=5	γ=10	γ=20	γ=50
0	0	61.849	62.256	62.928	63.856	65.027	73.985	101.479	204.458
	1	62.051	63.051	64.679	66.881	69.595	88.607	138.406	303.581
	2	62.251	63.834	66.375	69.752	73.829	100.758	166.198	375.323
	3	62.451	64.606	68.021	72.487	77.790	111.349	189.443	435.356
	4	62.650	65.367	69.620	75.104	81.520	120.850	209.841	487.473
	5	62.848	66.117	71.177	77.615	85.055	129.535	228.240	534.387
1	0	51.460	53.093	55.705	59.165	63.331	90.742	157.650	372.655
	1	52.074	55.431	60.607	67.174	74.754	120.276	222.390	539.644
	2	52.680	57.673	65.134	74.303	84.610	143.740	271.970	665.872
	3	53.279	59.829	69.358	80.790	93.404	163.813	313.753	771.718
	4	53.871	61.908	73.333	86.779	101.418	181.644	350.563	864.708
	5	54.457	63.918	77.097	92.370	108.828	197.853	383.843	948.620
2	0	51.435	54.264	58.671	64.325	70.919	111.275	203.124	489.886
	1	52.458	58.044	66.299	76.336	87.523	150.833	286.776	703.061
	2	53.461	61.589	73.118	86.660	101.380	181.837	350.892	865.203
	3	54.445	64.937	79.339	95.850	113.515	208.205	404.933	1001.310
	4	55.412	68.117	85.095	104.210	124.444	231.551	452.544	1121.557
	5	56.361	71.151	90.475	111.932	134.465	252.726	495.590	1229.764
3	0	51.697	55.677	61.733	69.306	77.938	128.566	239.979	583.846
	1	53.120	60.789	71.735	84.654	98.742	176.048	338.856	834.566
	2	54.504	65.494	80.473	97.556	115.775	213.042	414.674	1026.409
	3	55.854	69.876	88.327	108.899	130.549	244.428	478.589	1186.773
	4	57.172	73.993	95.520	119.127	143.775	272.179	534.902	1328.341
	5	58.459	77.886	102.192	128.540	155.857	297.327	585.818	1456.250
4	0	52.033	57.124	64.706	73.993	84.398	143.743	271.798	664.603
	1	53.846	63.473	76.824	92.237	108.798	197.993	383.815	947.830
	2	55.598	69.229	87.230	107.341	128.531	240.121	469.735	1164.346
	3	57.296	74.530	96.487	120.515	145.547	275.816	542.171	1346.469
	4	58.945	79.468	104.907	132.348	160.730	307.355	605.995	1506.793
	5	60.547	84.108	112.679	143.181	174.568	335.922	663.703	1651.661

(*)Results obtained using the absolute nodal coordinate formulation and 10 elements

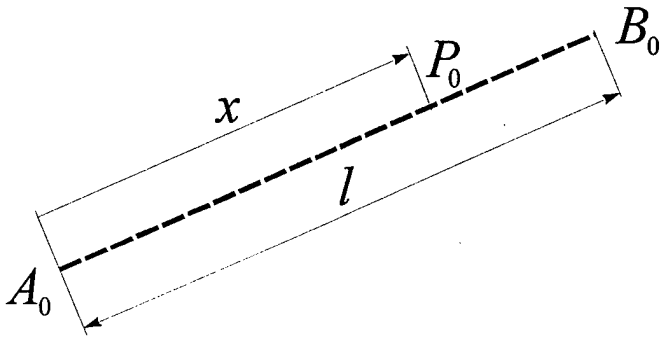

a) Undeformed configuration

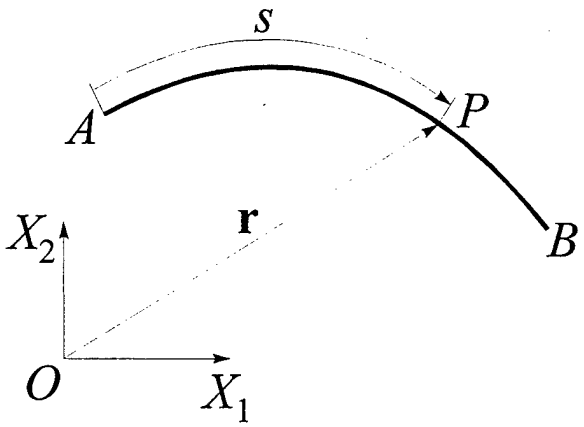

b) Current (deformed) configuration

Fig. 1. Undeformed (reference) and current configurations in the absolute nodal coordinate formulation.

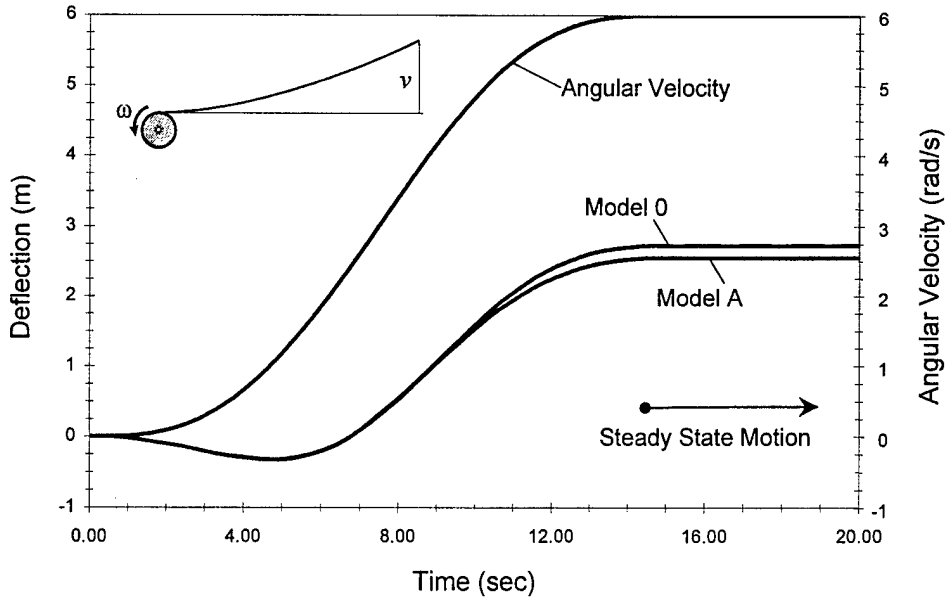

Fig. 2. Angular velocity and tip deflection results in the spin-up maneuver of an eccentrically suspended beam obtained using the absolute nodal coordinate formulation with 2 elements.

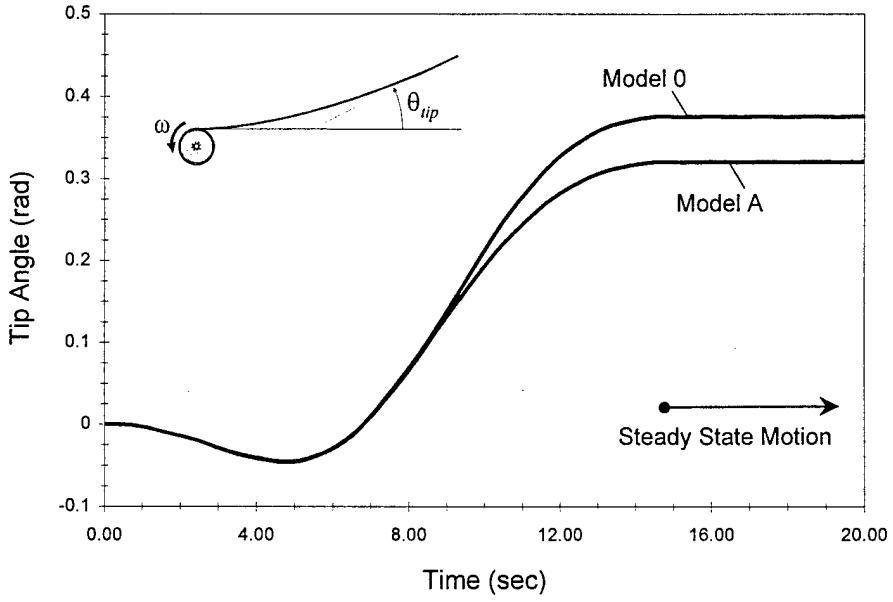

Fig. 3. Rotation of the free end predicted for the spin-up maneuver of an eccentrically suspended beam using the absolute nodal coordinate formulation and 2 elements.

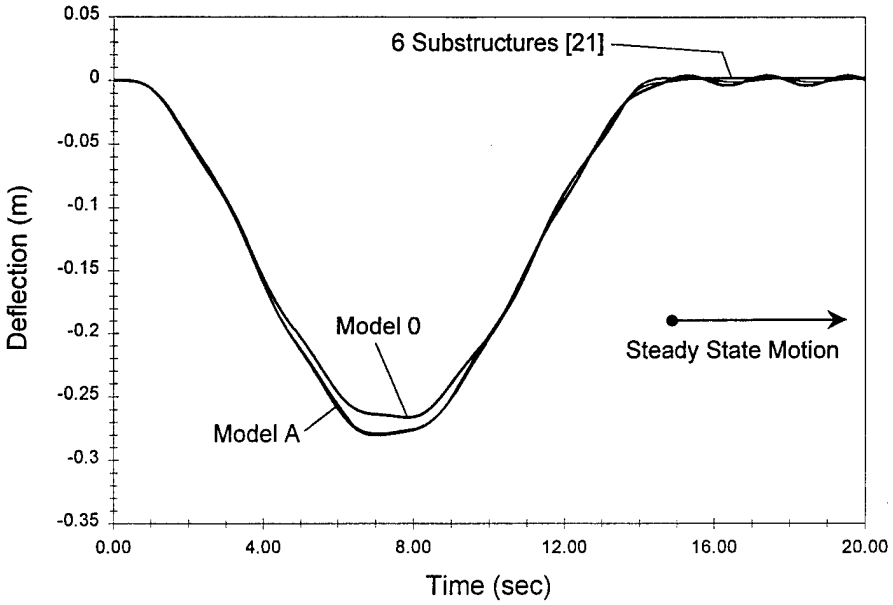

Fig. 4. Tip deflection in the spin-up maneuver of a rotating beam (steady-state angular velocity = 2 rad/s).

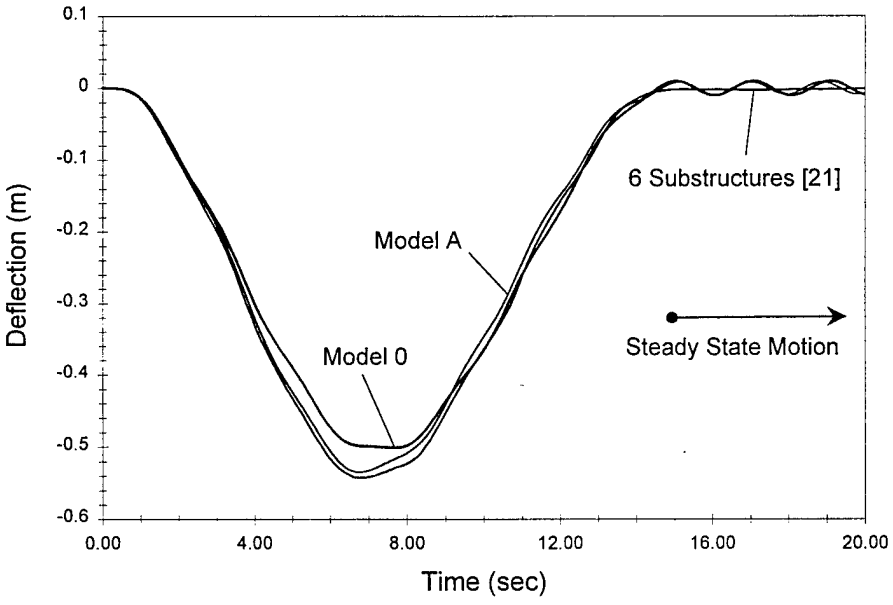

Fig. 5. Tip deflection in the spin-up maneuver of a rotating beam (steady-state angular velocity = 4 rad/s).

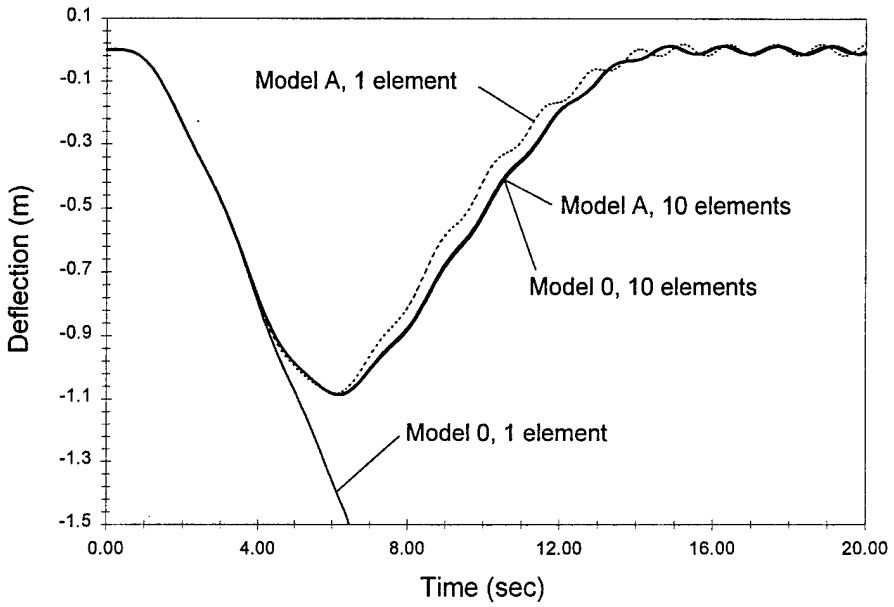

Fig. 6. Tip deflection in the spin-up maneuver of a rotating beam (steady-state angular velocity = 10 rad/s).

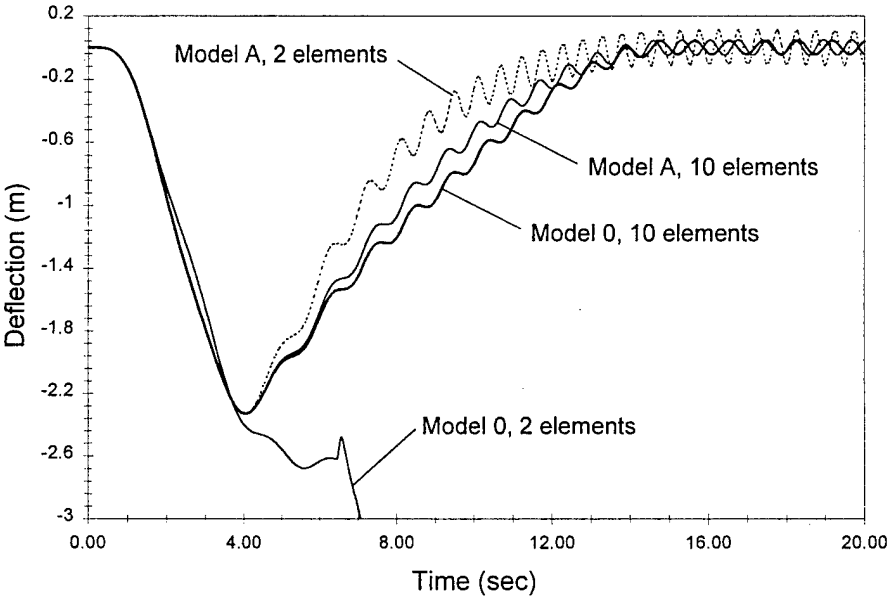

Fig. 7. Tip deflection in the spin-up maneuver of a rotating beam (steady-state angular velocity = 40 rad/s).

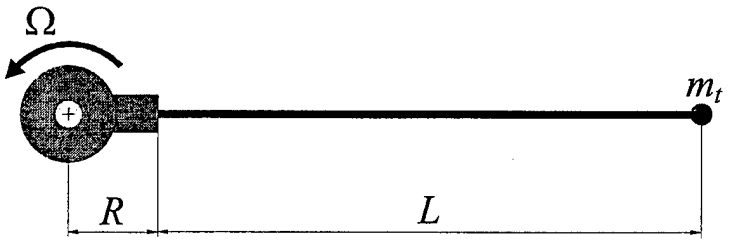

Fig. 8. Rotating cantilever beam attached to a rigid hub with a tip mass.

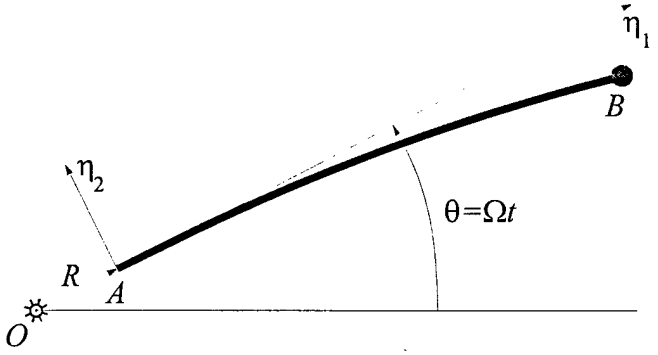

Fig. 9. Rotating coordinate system.

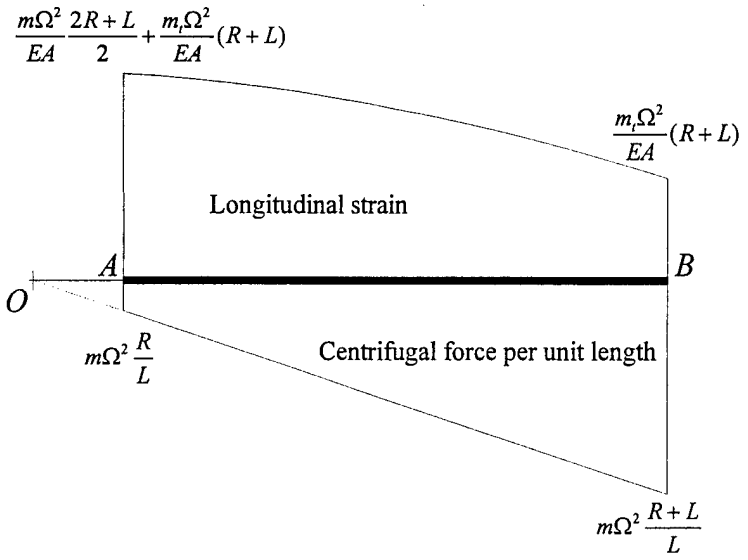

Fig. 10. Centrifugal force and longitudinal strain of the rotating cantilever beam.

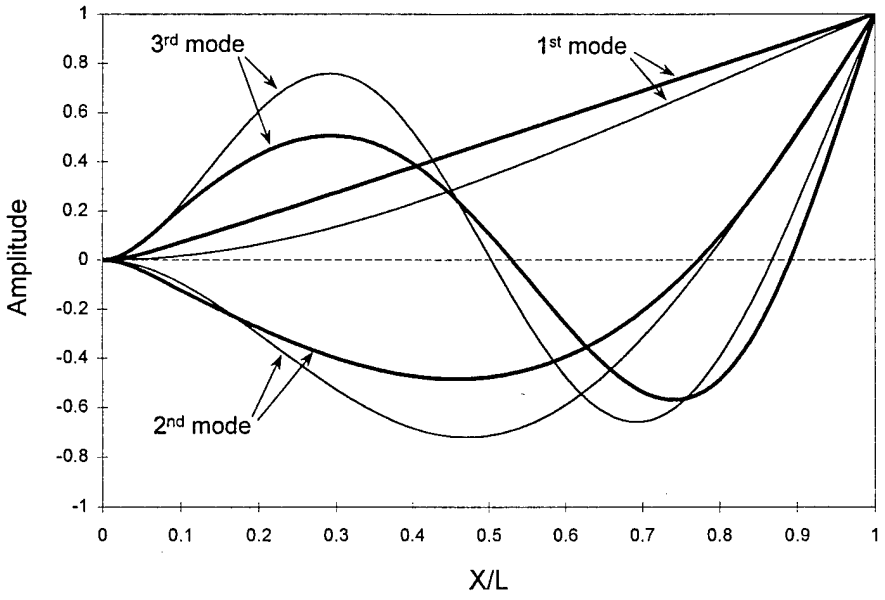

Fig. 11. First three transverse mode shapes when R=0 and m_t=0 for different values of the non-dimensional angular velocity: — γ=0; — γ=50.

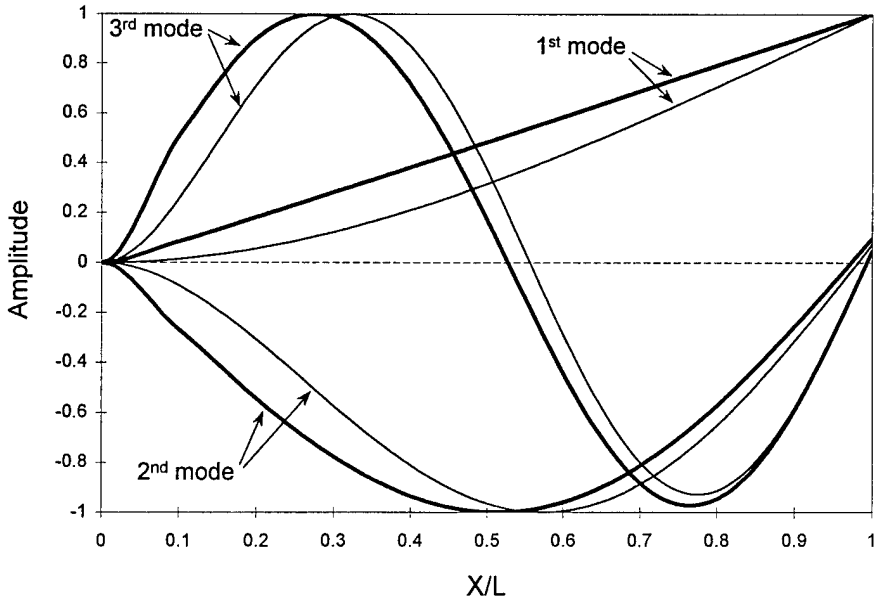

Fig. 12. First three transverse mode shapes when $R=2L$ and $m_t=3m$ for different values of the non-dimensional angular velocity: — $\gamma=0$; — $\gamma=50$.

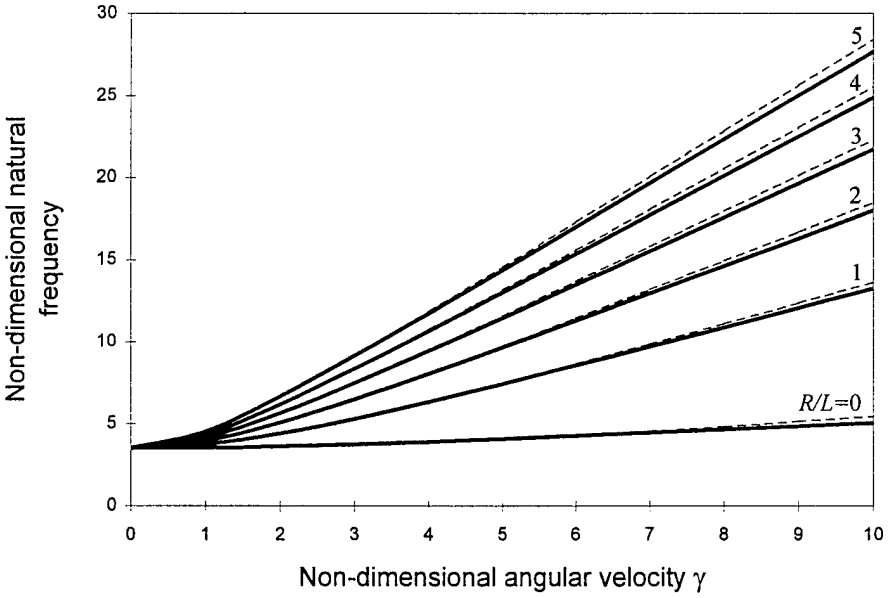

Fig. 13. Natural frequency of the first transverse mode for different values of R/L: — Simulation results; – – Approximate formula.

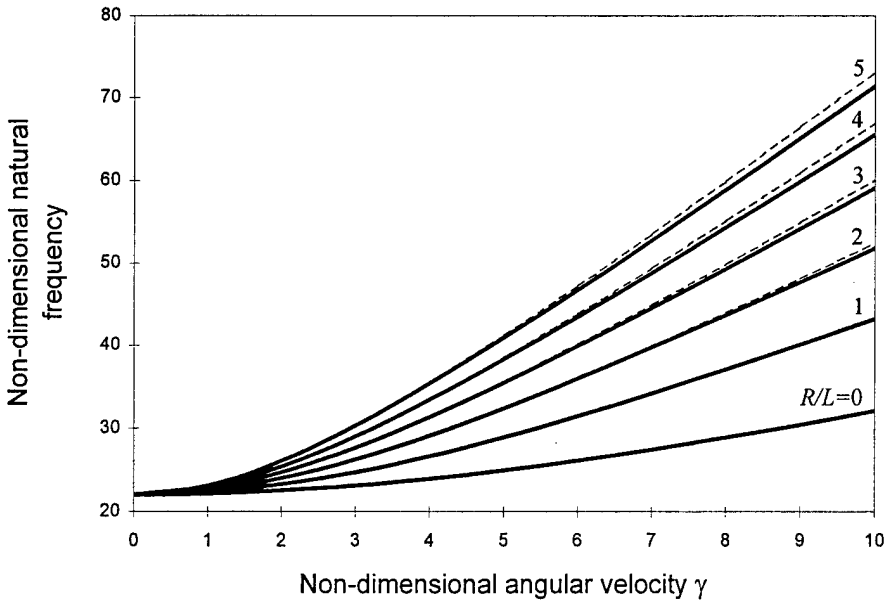

Fig. 14. Natural frequency of the first transverse mode for different values of *R/L*: — Simulation results; – – Approximate formula.